Effect of Initial Buffer Composition on pH Changes During Far-From-Equilibrium Freezing of Sodium Phosphate Buffer Solutions

Gerardo Gómez,[1] Michael J. Pikal,[2,3] and Naír Rodríguez-Hornedo[4]

Purpose. This study aims to assess the pH changes induced by salt precipitation during far-from-equilibrium freezing of sodium phosphate buffers as a function of buffer composition, under experimental conditions relevant to pharmaceutical applications—sample volumes larger than a few microliters, experiencing large degrees of undercooling and supersaturation.

Methods. Buffer solutions were prepared by dissolving the monosodium and disodium phosphate salts in the appropriate ratios to obtain initial buffer concentrations in the range of 8–100 mM and pH values between 5.7 and 7.4 at 25°C. Temperature and pH were monitored *in situ* during cooling to −10°C (at a rate of 0.3 to 0.5°C/min) and for 10–20 min after the sample reached the final temperature. Salt crystallization was confirmed by ion analysis and x-ray powder diffraction.

Results. Precipitation of $Na_2HPO_4 \cdot 12H_2O$ caused abrupt pH decreases after the onset of ice crystallization, at temperatures between −0.5 and −4.0°C. Decreasing the initial buffer concentration and/or initial pH resulted in higher final pH values at −10°C, farther removed from the equilibrium value of 3.6. At an initial pH of 7.4, the 50 and 100 mM buffer solutions reached a pH of 4.2 ± 0.1 at −10°C, whereas the 8 mM solutions reached a pH of 5.2 ± 0.2. Solutions having an initial pH of 5.7 and initial buffer concentrations of 8 and 100 mM experienced less pH shifts upon freezing to −10°C, with final pH values of 5.1 ± 0.1 and 4.7 ± 0.1, respectively.

Conclusions. Precipitation-induced pH shifts are dependent on the concentrations (activities) of precipitating ions, and are determined by both initial pH and salt concentration. The ion activity product is a meaningful parameter when describing salt precipitation in solutions prepared by mixing salts containing precipitating and nonprecipitating ions.

KEY WORDS: freezing; freeze-drying; salt precipitation; pH changes; phosphate buffers.

INTRODUCTION

Solutions of sodium phosphates are commonly used as buffers in pharmaceutical formulations to be freeze-dried. However, their use for this purpose is problematic due to the potentially massive drop in pH that may arise during the freezing stage of the freeze-drying process caused by the precipitation of $Na_2HPO_4 \cdot 12H_2O$ (1–4). The importance of pH in determining the stability of proteins (5,6), antibiotics (7), and sugars (8) in frozen and freeze-dried formulations has been reported. Stability problems during freezing, freeze-drying, and storage of formulations may be encountered if the pharmacologically active compound, or one of the excipients in the formulation, undergoes irreversible inactivation or chemical degradation at pH values different from the original pH at which the formulation was prepared.

The pH changes of sodium phosphate buffers during freezing at close-to-equilibrium conditions have been thoroughly studied (1,9). However, it is recognized that during actual freezing or freeze-drying operations, one does not operate close to equilibrium regarding either nucleation and initial crystal growth of ice or the nucleation and crystal growth of solute species (2,10–12). During far-from-equilibrium freezing, equilibrium behavior will be approached if the precipitation rate of the solute is fast on the time scale of cooling, so that the supersaturation levels remain small and roughly constant during cooling. However, supersaturation levels will be large when the solute precipitation rate is slow during cooling. In the latter case, the fraction of solute crystallized will be less than the equilibrium value. Thus, although studies carried out near equilibrium do provide a useful "baseline" set of observations, it is really observations of the phase behavior of systems far from equilibrium that are capable of providing generalizations of practical utility. A very important question that remains unanswered is how do the variables that control salt precipitation regulate the pH and extent to which buffer salts precipitate during far-from-equilibrium freezing.

Previous studies to investigate pH changes during freezing and the precipitation phenomena that cause them vary widely with regard to the variables that influence salt precipitation, specifically salt concentration, cooling rate, temperature, and solution volume. Van den Berg and Rose (1) investigated the crystallization-induced pH changes during freezing of 20 mM phosphate buffers at close-to-equilibrium conditions where both ice and salt crystallize at low undercooling and supersaturation. This was achieved by cooling solutions (125 ml) at a slow rate (less than 2°C/h) and by seeding with a small amount of the same frozen solution at temperatures just below the freezing point ($\Delta T < 1°C$). They report that disodium phosphate dodecahydrate is the least soluble salt in the sodium phosphate buffer (eutectic temperature = −0.5°C and eutectic concentration = 0.11 M), and that it precipitates first at initial pH values greater than 3.6 (at monosodium to disodium phosphate molar ratios below 3.42/0.06). Murase et al. (2,3) studied salt precipitation during nonequilibrium freezing of phosphate solutions, 10 mM and ≥200 mM, by calorimetry and by electron microscopy. Solution volumes in the range of 2–5 μl were cooled at rates of 0.62°C/min to −5°C and 10^3 °C/min to −196°C. Precipitation of $Na_2HPO_4 \cdot 12H_2O$ was found to be concentration dependent. Precipitation of $Na_2HPO_4 \cdot 12H_2O$ readily occurred at disodium phosphate salt concentrations ≥200 mM, whereas no salt precipitation was detected at concentrations ≤10 mM. Cavatur and Suryanarayanan (4) identified the crystalline phases formed during nonequilibrium freezing of sodium

[1] Present address: Dupont Pharmaceuticals, Manatí, Puerto Rico 00674.

[2] Eli Lilly & Co., Indianapolis, Indiana 46285.

[3] Present address: School of Pharmacy, University of Connecticut, Storrs, Connecticut 06269.

[4] College of Pharmacy, University of Michigan, Ann Arbor, Michigan 48109-1065.

[5] To whom correspondence should be addressed. (e-mail: nrh@umich.edu)

phosphate buffers at concentrations $\geq$190 mM, where solution volumes of 300 μl were cooled at a rate of ~15°C/min to −40°C. Precipitation of the monosodium phosphate salt has not been observed during nonequilibrium freezing (2–4), even with concentrations as high as 1.42 M (4). So far, salt precipitation and pH changes in sodium phosphate buffer solutions induced by freezing have been reported either at close-to-equilibrium conditions in large volumes, or at far-from-equilibrium conditions in small volumes. The present study reports changes in pH measured *in-situ* during far-from-equilibrium freezing, at conditions similar to those used in freeze-drying of pharmaceutical products, cooling rates in the range of 0.3–0.5°C/min, volumes of approximately 25 ml, and initial buffer concentrations in the range of 8–100 mM.

Knowledge of ion concentrations (activities) and ion products is instrumental to understanding the influence that initial buffer composition and pH have on salt precipitation and pH during freezing of solutions of nonstoichiometric composition (13–15). The factors that influence the precipitation of $Na_2HPO_4 \cdot 12H_2O$ will determine the pH of the unfrozen solution during nonequilibrium freezing of buffer solutions. These include the ion product, supersaturation, rate at which supersaturation is created, solubility of $Na_2HPO_4 \cdot 12H_2O$, presence of additives, temperature, and volume and viscosity of the interstitial solution. The aim of the research presented here is to explain the effects that undercooling of solutions and initial buffer composition have on the precipitation-induced pH changes during far-from-equilibrium freezing of sodium phosphate buffer solutions. This was achieved by monitoring the pH and temperature of solutions containing the sodium phosphate buffer during far-from-equilibrium freezing to −10°C. Crystallization of phosphate salts was correlated with pH shifts by calculating the phosphate speciation corresponding to the measured pH, and was validated by ion analysis of freeze concentrates and x-ray diffraction analysis after freeze-drying. The effects that supersaturation and additive concentration have on salt precipitation and pH will be presented in subsequent publications.

MATERIALS AND METHODS

Materials

Monosodium hydrogen phosphate monohydrate ($NaH_2PO_4 \cdot H_2O$) was obtained from Mallinckrodt (St. Louis, MO) and disodium hydrogen phosphate (Na_2HPO_4) was obtained from J.T. Baker (Phillipsburg, NJ). Both salts were used without further purification. Deionized water was used throughout all the experiments. Technical buffers (Radiometer, no. 943-111 and 943-112, Westlake, OH) having pH values of 4.01 and 7.00 were used for the calibration of the electrode and pH meter. A low-temperature buffer (Radiometer, No. S 1366) having a pH value of 6.40 at −10°C was used to verify the calibration at sub-zero temperatures.

Preparation of Buffer Solutions

Buffer solutions were prepared by dissolving the monosodium and disodium phosphate salts in the appropriate ratios to obtain the desired pH values in the range of 5.7 to 7.4 at 25°C and buffer concentrations (C_{TP_i}) between 8 and 100 mM. Table 1 summarizes the initial pH and composition of

Table 1. Initial pH and Composition of Buffer Solutions at 25°C

Solution	pH	C_{TP}^a (mM)	Ion concentration (mM)		
			Na^+	HPO_4^{2-}	$H_2PO_4^-$
A	7.4	100	181	81	19
B	7.4	50	88	38	12
C	7.4	20	35	15	5
D	7.4	8	14	6	2
E	6.7	100	148	48	52
F	6.7	8	11	3	5
G	5.7	100	106	6	94
H	5.7	8	8.4	0.3	7.7

^{a} Total phosphate concentration.

buffer solutions. All solutions were filtered through a type HA filter (Millipore) of 0.45 μm pore size.

Temperature and pH Measurements During Freezing

The buffer solution (25 ml) was placed in a 30-ml beaker and kept inside a temperature circulator (Lauda, RLS 6-D, Konigshofen, Germany). A combined electrode (Ingold, Lot 401 57 60, Wilmington, MA) was placed in the center of the sample and connected to a pH meter (Radiometer, PHM 85, Westlake, OH) to monitor the electromotive force, EMF. The ability of this electrode to operate at sub-zero temperatures relies on two distinctive features: the high electrical conductivity of its glass membrane ($\approx 10^{-9}$ S/cm at 25°C) (16), which improves the response time at lower temperatures, and the use of a reference electrolyte containing glycerol (Fryscolyte "B"™), which allows measurements to −30°C. The presence of glycerol also reduces the liquid junction potential, resulting in highly reproducible pH measurements. A copper-constantan thermocouple (0.02 in. diameter; Omega, TMQSS-020G-6, Stamford, CT) connected to a digital readout (accuracy of 0.2°C; Omega DP-41) was used to monitor the temperature of the sample. The thermocouple was placed directly below the pH electrode and in contact with the glass membrane. Temperature readings from the thermocouple-indicator were checked with those from the temperature circulator and found to agree within 0.1°C.

The solutions were allowed to equilibrate to 0°C, after which the temperature of the sample was lowered at a rate of 0.3–0.5°C/min until spontaneous ice nucleation took place. The circulator temperature was then set to −10°C immediately following ice nucleation. Throughout the experiment both the temperature and EMF of the solution were monitored, and the data were automatically collected by a computer (IBM PC XT). A computer program was written to lower the bath temperature at the desired rate (before ice nucleation) and to maintain the bath temperature at −10°C after ice nucleation. Data were collected until about 10 min after the frozen sample reached −10°C. The pH of the solution was calculated from the measurements of EMF and temperature (17).

Ion Analysis of Residual and Interstitial Solutions

Freezing proceeded in radial fashion, from the beaker wall toward the center. Samples of residual and interstitial solution were removed from the center of the beaker during freezing and from the interstitial spaces between the ice dur-

ing warming, respectively. For the residual solution samples, approximately 0.1 ml was removed with a pipette at 10, 15, and 22 min after the onset of ice nucleation. This procedure was carried out on a concentrated buffer ($C_{TP_i} = 100$ mM) and a dilute buffer ($C_{TP_i} = 8$ mM) with initial pH of 7.4 at 25°C. All samples were weighed, diluted, and analyzed for sodium and total phosphate content by inductively coupled plasma (Leeman Labs, Plasma III, Hudson, NH).

Interstitial solution samples were obtained after freezing buffer solutions to −10°C for about 10 min and warming to temperatures in the range of −3 to −1°C. Samples were removed through a 21-gauge needle that was inserted in the center of the beaker at the beginning of the experiment. Throughout the experiment, a positive pressure was maintained in the needle to prevent solution freezing inside the needle. Because of the small volumes of interstitial solution present in this temperature range, a vacuum pump was used to withdraw the samples. Small volumes (20–100 μl) were collected in the hose connecting the needle to the pump. Attempts to remove samples from the 8mM buffer solutions were unsuccessful because of the very small volumes of interstitial solution.

X-ray Powder Diffraction of Freeze-Dried Buffer Solutions

With the objective of identifying the crystalline phases that form during freeze-drying, freeze-dried sodium phosphate buffers were analyzed by X-ray powder diffraction (Siemens, D5000 system with Cu-K$_\alpha$ radiation, 50 kV, 40 mA, New York, New York). Twenty-five milliliters of the appropriate buffer solution was freeze-dried in a Virtis (New York, New York) 25 SRC-X freeze-drier. Shelf temperature was initially −5°C, and after thermal equilibration with the solution in the vials, the shelf temperature was lowered to −30°C. The solutions were undercooled by approximately 15°C. The shelf temperature was then lowered to −45°C, and freezing was complete in about 4 h. The temperature of the frozen solution was maintained between −30 and −35°C for the duration of primary drying (68 h). Secondary drying was done at 30°C and lasted 18 h.

RESULTS

Characterization of Frozen System

The predominant mechanism for the freezing of the buffer solutions examined in this study is by directional solidification; that is, ice growth takes place from a moving interface from the walls of the beaker toward the center (18). Figure 1 shows a typical temperature distribution within the buffer solution as a function of time. From the beginning of the experiment at t = 0 until t = 22 min, the entire volume of solution is undercooled. Only the uppermost layer of the solution which is in contact with air (location no. 4) shows a 2°C temperature lag relative to the rest of the solution. At t = 22 min ice nucleates uniformly throughout the solution, raising the temperature of the entire volume to −0.5°C. The release of the latent heat of crystallization is the limiting factor for the new ice crystals to grow, and visual inspection shows that an ice front develops and immediately moves away from the walls of the beaker. A sudden drop in temperature results when the front reaches the thermocouple. Freezing is com-
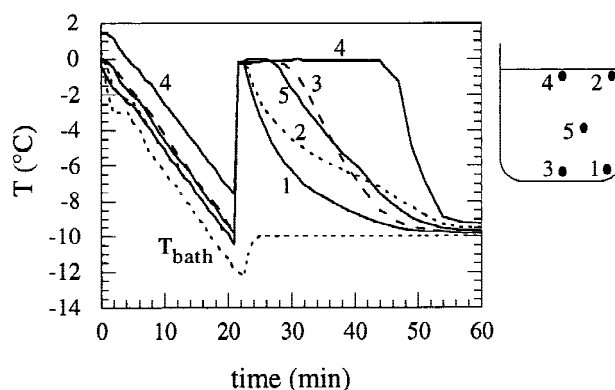

Fig. 1. Temperature distribution in the beaker during nonequilibrium freezing of sodium phosphate buffer solutions, $C_{TP_i} = 100$ mM, pH$_i$ 7.4 at 25°C. The number on the curve indicates the location of the thermocouple within the beaker as represented on the side diagram.

plete when the front reaches location no. 4 at about 25 min after the onset of ice nucleation. The presence of the pH electrode in the solution did not affect the evolution of the moving interface based on results of experiments with and without the electrode.

To assess the extent of solute rejection by the ice front, the sodium and total phosphate concentrations were measured in the residual solution in the center of the beaker after the onset of ice crystallization, in buffers with an initial pH of 7.4 at 25°C. As shown in Fig. 2, the most dilute buffer solution, $C_{TP_i} = 8$ mM (solution D in Table 1), experienced larger
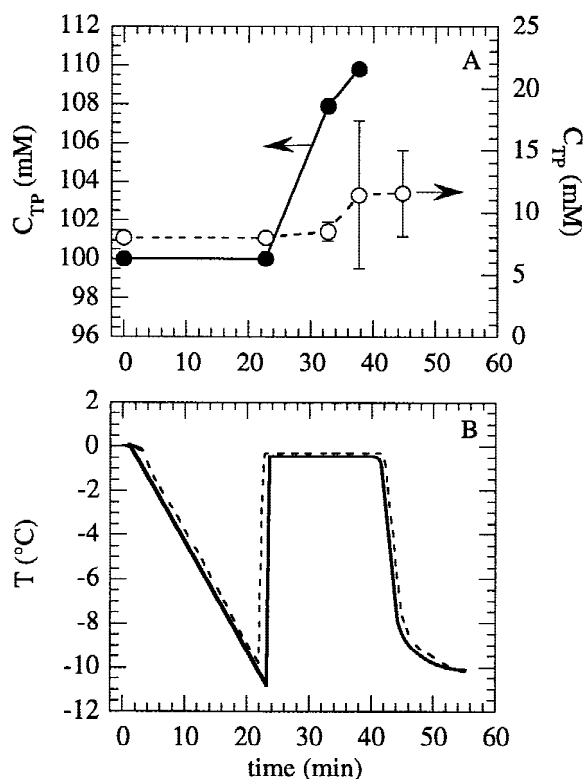

Fig. 2. (A) Buffer concentration in the center of the beaker during nonequilibrium freezing of buffer solutions, C_{TP_i} of 8 mM (○) and 100 mM (●), and initial pH of 7.4 (25°C). (B) Temperature-time profile in the center of the beaker for the above buffer solutions 8 mM (---) and 100 mM (—).

relative increases in buffer concentration and greater variability in these values during freezing than the most concentrated buffer, $C_{TP_i} = 100$ mM (solution A in Table 1). A comparison of these results with those during close-to-equilibrium freezing of a phosphate buffer is presented in Figure 3. The concentration of phosphate can increase 150-fold during close-to-equilibrium freezing of a buffer with C_{TP_i} of 20 mM to −9.9°C. It is observed that decreasing the initial buffer concentration increases the departure from equilibrium behavior, i.e., C_{TP} for 8 mM is much less than the equilibrium line or the 100 mM data. Even though at −0.5°C the C_{TP} at equilibrium is 150 mM, C_{TP} values only as high as 17 mM were achieved during far-from-equilibrium freezing of buffers with C_{TP_i} of 8 mM.

Ion concentrations of interstitial solutions embedded in the ice matrix (Table 2) show that these experienced a much larger increase in concentration than residual solutions (Fig. 3), which caused precipitation of $Na_2HPO_4 \cdot 12H_2O$ and a decrease in pH. Evidence of this precipitation is shown for a buffer solution having an initial pH of 7.4 at 25°C and initial buffer concentration of 100 mM (Table 2). The sodium-to-total-phosphate molar ratio, C_{Na}/C_{TP}, was calculated from the ion analysis of the interstitial solution. The pH was then computed (pH_{IA}) from ionic equilibrium expressions (Eqs. 1–4) coupled to mass and charge balances (Eqs. 5 and 6):

$$a_{H^+} a_{H_2PO_4^-} = K_{a_1} a_{H_3PO_4} \tag{1}$$

$$a_{H^+} a_{HPO_4^{2-}} = K_{a_2} a_{H_2PO_4^-} \tag{2}$$

$$a_{H^+} a_{PO_4^{3-}} = K_{a_3} a_{HPO_4^{2-}} \tag{3}$$

$$a_{H^+} a_{OH^-} = K_W \tag{4}$$

$$m_{H_3PO_4} + m_{H_2PO_4^-} + m_{HPO_4^{2-}} + m_{PO_4^{3-}} = m_{TP} \tag{5}$$

$$m_{H^+} + m_{Na^+} = m_{H_2PO_4^-} + 2m_{HPO_4^{2-}} + 3m_{PO_4^{3-}} + m_{OH^-} \tag{6}$$

where a denotes activity, K_a is the acid dissociation constant, K_w is the water dissociation constant, m is the concentration in molality, and m_{TP} is the total phosphate molality. The decrease in the values of C_{Na}/C_{TP} and measured pH (pH_{EMF}) indicate precipitation of $Na_2HPO_4 \cdot 12H_2O$. There is good agreement between the pH values calculated by both methods: ion analysis and EMF measurements (Table 2), and between the C_{TP} values during warming and at equilibrium (Fig. 3).

Table 2. Interstitial Solution Composition and pH of Sodium Phosphate Buffer Having an Initial Buffer Concentration of 100 mM and Initial pH of 7.4 at 25°C (solution A)

Exp. no.	T (°C)	C_{Na}/C_{TP}	C_{TP}(mM)	pH_{IA}^a	pH_{EMF}^b
1	−3.0	1.19	539	6.1	5.8
2	−3.0	1.14	681	5.9	5.8
3	−3.0	1.20	609	6.0	5.8
	−2.5	1.24	574	6.2	6.0
	−1.0	1.36	371	6.5	6.7
4	−2.5	1.19	621	6.0	6.0
	−2.5	1.19	628	6.1	6.0
	−2.5	1.30	613	6.3	6.0

[a] pH calculated from ion concentration measurements with inductively coupled plasma.
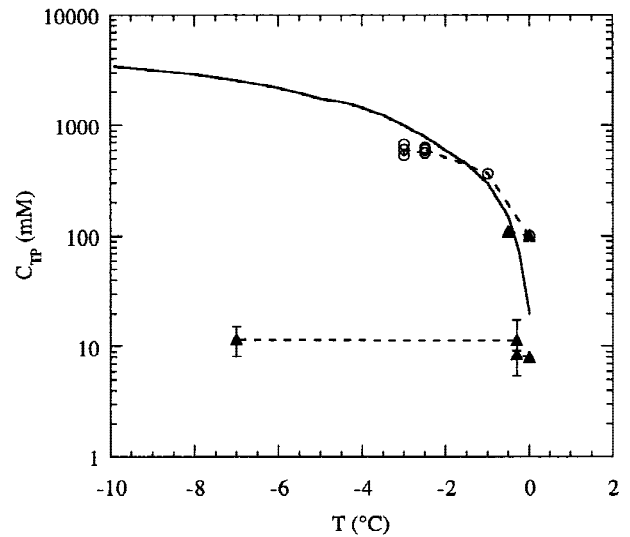[b] pH calculated from EMF measurements with pH electrode.

Fig. 3. Comparison of total phosphate concentration, C_{TP}, during equilibrium and nonequilibrium freezing of sodium phosphate buffers with initial pH of 7.4 (25°C): equilibrium freezing, after (1), (—); nonequilibrium freezing, residual solution (--▲--); and during warming after nonequilibrium freezing to −10°C for 10 min, interstitial solution (--○--).

Water Undercooling and pH During Freezing

The behavior of sodium phosphate buffer solutions having an initial pH of 7.4 (25°C) and initial C_{TP} of 100 mM (solution A) during nonequilibrium freezing is shown in Fig. 4. Initially, the buffer solution cools at the same rate as the bath until freezing of water occurs. Undercooling of water ranged from 5 to 12°C and was independent of initial buffer concentration and initial pH. The latent heat evolved during ice crystallization warmed the sample to temperatures between −0.5 and −0.1°C, after which the sample cooled to the bath temperature of −10°C. Small pH increases of ≤0.5 units were observed while solutions supercooled, before ice nucleation occurred. During ice crystallization, as the buffer concentration and ionic strength increased, the pH of the unfrozen solution decreased by ≤1 unit. These events were followed by a sharp decrease in pH at temperatures between −0.5 and −4°C, and by pH values at −10°C of at least 3.4 units lower than the original solution (pH 7.4, 25°C). This large drop in pH is due to the change in ratio of the dissolved phosphate salts as a consequence of $Na_2HPO_4 \cdot 12H_2O$ precipitation. This was confirmed by measuring ion compositions of the unfrozen solution and by X-ray powder diffraction of the freeze-dried buffers. Crystalline NaH_2PO_4 was not detected. These results show that precipitation of $Na_2HPO_4 \cdot 12H_2O$ and the resulting pH behavior during freezing were not significantly affected by the range of water undercoolings experienced by these solutions.

Initial Buffer Concentration and Initial pH

The initial buffer concentration and initial pH determine the concentration of ions that participate in the precipitation of $Na_2HPO_4 \cdot 12H_2O$, and thus the supersaturation with respect to this salt. The pH and temperature of buffer solutions having initial pH values between 7.4 and 5.7 (25°C) were monitored during freezing. The initial pH and concentrations
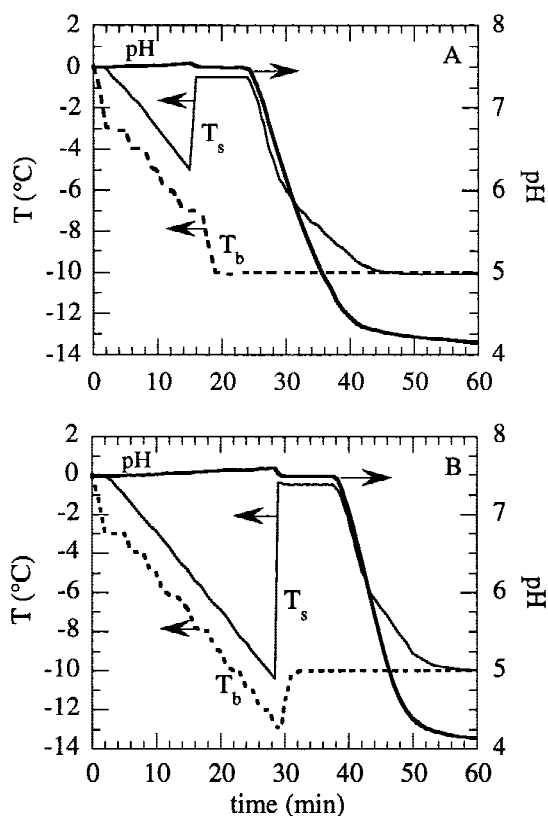
Fig. 4. Effect of water undercooling, ΔT_w, on pH during nonequilibrium freezing of sodium phosphate buffer solutions ($C_{TPi} = 100$ mM, pH_i 7.4 at 25°C). T_s is the temperature of the solution adjacent to the electrode and T_b is the temperature of the heat sink (bath) temperature. (A) $\Delta T_w = 4.6°C$; (B)$\Delta T_w = 9.8°C$.

of buffer solutions are shown in Table 1. All solutions were hypoeutectic. The highest initial concentration of the least soluble salt, Na_2HPO_4, at $C_{TP_i} = 100$ mM and pH 7.4, was 81 mM, which is 26% lower than the binary eutectic composition of 110 mM. The temperature at which spontaneous nucleation of $Na_2HPO_4 \cdot 12H_2O$ occurs (Tp) was essentially independent of initial buffer concentration for $C_{TP_i} \geq 20$ mM, with a range of Tp between −0.5 and −0.7°C. With the more dilute buffer, $C_{TP_i} = 8$ mM, there was a wider variability in Tp, with values in the range of −0.5 to −4°C. Because the nucleation rate of the salt often exhibits an exponential dependence on supersaturation (15,19,20), there is a concentration threshold below which greater undercoolings and higher supersaturations during freeze concentration are required for spontaneous nucleation to occur.

The dependence of pH at −10°C on the initial pH and initial buffer concentration is summarized in Fig. 5. Decreasing initial pH in the range of 7.4–5.7, while maintaining the buffer concentration constant, decreases the concentration of the less soluble salt, $Na_2HPO_4 \cdot 12H_2O$, relative to NaH_2PO_4. Although lower pH values at −10°C were achieved by the more concentrated buffer solutions (C_{TP_i} 100 mM compared with 8 mM), the pH upon freezing to −10°C was independent of initial pH for all conditions studied (solutions A, E, D, F, and H), except for the 100 mM buffer with initial pH of 5.7 (solution G). Compared with the behavior of 100 mM buffer solutions at higher initial pH, the pH at −10°C was less acidic for solutions with an initial pH of 5.7. This corresponds to a
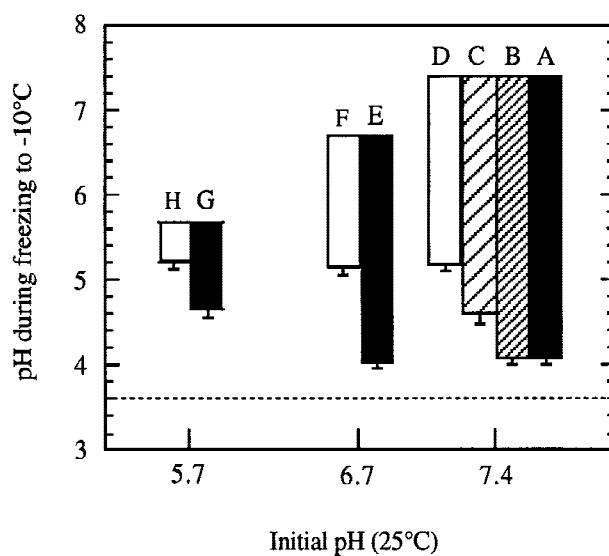

Fig. 5. Effect of initial pH and initial buffer concentration on the pH of sodium phosphate buffer solutions during nonequilibrium freezing to −10°C. The letters above the bars refer to the solutions in Table 1. $C_{TP_i} = 8$ mM ($\square$), 20 mM ($\boxslash$), 50 mM ($\boxbslash$), and 100 mM ($\blacksquare$). Equilibrium pH at −10°C, after reference 1, (- - -).

decrease in the fraction of $Na_2HPO_4 \cdot 12H_2O$ precipitated when the initial pH is decreased from 6.7 to 5.7.

Ion Activity Product

Under nonequilibrium freezing conditions, the monosodium phosphate rarely crystallizes (2–4), and pH decreases are a result of the crystallization of $Na_2HPO_4 \cdot 12H_2O$. Crystallization of electrolytes can be correlated with the solution composition and is dependent on the supersaturation with respect to the constituent ions (13,15,19). The supersaturation (σ) with respect to $Na_2HPO_4 \cdot 12H_2O$ at any pH is dependent on the ratio between the ion product (IP) and the solubility product (K_{sp}),

$$\sigma = \left(\frac{IP}{K_{sp}} \right)^{1/3} - 1 = \left(\frac{a_{Na^+}^2 \, a_{HPO_4^{2-}} \, a_{H_2O}^{12}}{a_{Na^+,eq}^2 \, a_{HPO_4^{2-},eq} \, a_{H_2O,eq}^{12}} \right)^{1/3} - 1$$

In the case of mixed salt systems, such as the buffers used in these studies, the composition of the solution must be expressed in terms of ion concentrations or activities and the supersaturation in terms of ion products. The buffers used in these studies were prepared by mixing salts containing indifferent ions and precipitating ions: $H_2PO_4^-$, Na^+ and HPO_4^{2-}, where the concentration of the sodium ion is altered by the salts used to prepare the buffer.

Although initial pH and initial buffer concentration are useful operational variables, it is difficult to interpret the results in terms of either variable alone because both variables are needed to determine ion concentrations and ion activities. Activities were estimated with the extended Debye-Hückel equation, and the required parameter values for these calculations were obtained from Kharaka et al. (21,22). Here, we focus on values of the ion product, IP. Calculation of supersaturations during freezing of sodium phosphate buffers will be presented in a subsequent publication (23).
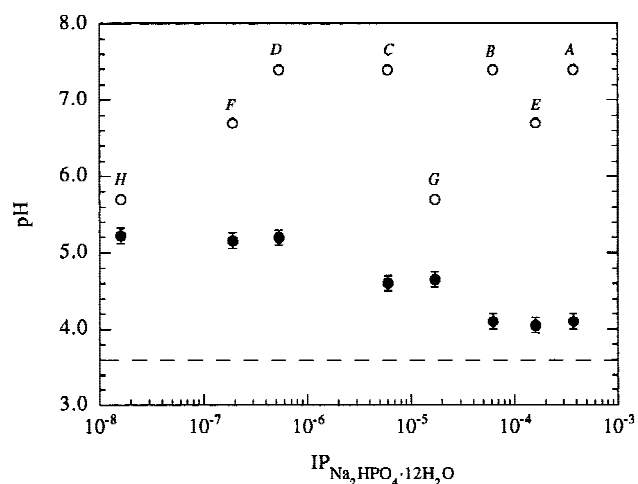
Figure 6 shows the dependence of the pH at −10°C on

Fig. 6. Effect of initial ion activity product of $Na_2HPO_4 \cdot 12H_2O$ on the pH of sodium phosphate buffer solutions upon freezing to $-10°C$. Letters (A–H) refer to solutions in Table 1. Initial pH at 25°C (○), pH at $-10°C$ (●), and equilibrium pH at $-10°C$, after reference 1, (---).

the initial ion activity product of $Na_2HPO_4 \cdot 12H_2O$. IPs are expressed on a molar basis and the initial water activity in these solutions was calculated to be between 0.995 and 1.000. These results reveal that for sodium phosphate buffers with $IP_{Na_2HPO_4 \cdot 12H_2O} \geq 6.2 \times 10^{-5}$, the pH at $-10°C$ reached the most acidic values, 4.1 ± 0.1, within 0.5 ± 0.1 pH units of the equilibrium value of 3.6. Less acidic pH values at $-10°C$, 5.2 ± 0.1, were obtained in the case of buffers with 1.6×10^{-8} $IP_{Na_2HPO_4 \cdot 12H_2O} \leq 5.3 \times 10^{-7}$.

DISCUSSION

On the basis of thermodynamic considerations, all of the buffer solutions studied were expected to reach a buffer concentration of 3.5 M and pH of 3.6 upon freezing to $-10°C$, if crystallization of ice and $Na_2HPO_4 \cdot 12H_2O$ had proceeded to equilibrium. In seeded systems, under near-equilibrium conditions, the pH and composition of the interstitial solution would have followed very closely the phase diagram reported by van den Berg and Rose (1). However, by freezing the buffer solutions at conditions far from equilibrium, where the systems experience large undercoolings and supersaturations, the resulting pH changes are determined by the rate and extent of crystallization of both ice and $Na_2HPO_4 \cdot 12H_2O$.

The events taking place during freezing include the nucleation process by which solid phases are formed and the modes by which crystal growth occurs. The driving force for the crystallization of the solvent and/or the solutes is the undercooling or the supersaturation with respect to the crystallizing phase(s). The rate of crystallization of the solvent will determine the freezing pattern, the channels or interstitial solution volume distribution, and the evolution of the solute concentration in the interstitial solution.

The undercooling of the solution will influence the size and morphology of the initial ice nuclei (11) which, upon growth, will eventually influence the size and shape of interstitial solution from which precipitation of $Na_2HPO_4 \cdot 12H_2O$ takes place. Thus, in principle, the undercooling of water could impact the subsequent salt crystallization and pH shifts.

In the present study, small variations in the undercooling (5–12°C) did not affect salt precipitation. This is because, in the experiments presented here, ice growth takes place mainly from an ice-liquid interface (front) advancing through the sample in a direction opposite to the heat sink, instead of growing from the initial ice nuclei. The morphology of this interface will be determined mainly by heat transfer parameters such as temperature of the heat sink (dashed line in Fig. 4) and radius of the beaker (24). These two factors remained constant in all of the experiments. In other words, the presence of the moving interface will mask any differences in the morphology of the frozen phase created by the different degrees of undercooling. In the absence of a freezing front, the morphology of the ice crystal network will be determined mainly by the initial ice nuclei, because they will grow to a much larger extent during the initial release of latent heat of crystallization, without being incorporated into a moving interface. In this case, the undercooling may exert an effect on the subsequent salt crystallization and pH changes.

Evolution of the ice-liquid interface is complex. Ice first forms on the inside walls of the beaker as needles or dendrites and further develops into a tree-like pattern with side branching (25). A concentrated layer will develop in the residual solution ahead of this irregular interface. Most of the solutes will be trapped between the ice branches to form the interstitial solution. Some will be rejected by the front toward the center of the beaker (26), causing an increase in buffer concentration (Fig. 2).

Various factors contribute to the precipitation rate of the salt and the ability to form and maintain supersaturated solutions. These include: solution composition (concentrations or activities of crystallizing ions, inert ions, or other additives), solubility of the crystallizing solute, viscosity of the solution, rate at which supersaturation is created, volume of unfrozen solution, and temperature.

Changes in the initial buffer concentration affect both the total ion concentrations and the ion activity products. These two parameters influence salt precipitation by different processes. In addition to the intrinsic effect of ion activity product on supersaturation, the initial total buffer concentration regulates the rate at which the ions are concentrated in the unfrozen phase by altering the concentration of ions that do not participate in the precipitation as well as the fraction of the water that freezes. Because an increase in the rate of supersaturation increases the supersaturation at which spontaneous nucleation occurs, decreasing the total buffer concentration will increase the tendency of $Na_2HPO_4 \cdot 12H_2O$ to remain in a supersaturated solution, leading to smaller extents of salt precipitation and pH changes.

An important factor contributing to the decreased salt precipitation with decreasing initial buffer concentration arises from the larger supersaturations induced by the formation of smaller and more finely dispersed volumes of interstitial solution during freezing, since there is more water available for crystallization. Dispersing a solution into discrete small volumes isolates heterogeneous nuclei within a fraction of the drops and reduces the probability of an entropy fluctuation of the magnitude necessary to produce a viable nucleus, making nucleation more difficult (27). Studies on the nucleation of ice (28) and salts (29) in droplets of aqueous solutions (diameters <10 μm) dispersed within an emulsion, show that nucleation occurs after very large undercoolings,

typically 40°C for ice nucleation and 80°C for salt precipitation. Indeed, some solutions and solvents fail to crystallize and cool to a glassy state. The solution volume at which nucleation rates become insignificant depends on the concentration of additives (catalytic nucleation sites), the solubility of the crystallizing solute, and the viscosity of the solution.

Precipitation and solidification in small droplets or liquid volumes involving emulsions have been studied to identify the nucleation processes (27), develop purification processes, and control particle size and morphology (30). The dependence of phosphate salt precipitation on initial salt concentration during nonequilibrium freezing has been studied and explained by Murase et al. (3) in terms of the volumes of the solution domains in the freeze-concentrates. Calorimetric and microscopic studies indicate that the fraction of $Na_2HPO_4 \cdot 12H_2O$ precipitated during freezing of phosphate solutions began to decrease with a decrease in the initial buffer concentration below 500 mM, at approximately 200 mM disodium phosphate concentration (2,3), and $Na_2HPO_4 \cdot 12H_2O$ salt precipitation was not observed at disodium salt concentrations below 10 mM. The lower concentration limit for $Na_2HPO_4 \cdot 12H_2O$ precipitation was higher than indicated by our results, i.e., we found that salt precipitation began to decrease at initial buffer concentrations below 20 mM, 15 mM disodium phosphate concentration, and salt precipitation was still significant at buffer concentrations as low as 8 mM, 0.3 mM disodium phosphate concentration. Samples were cooled at a rate of 0.62°C/min, similar to the cooling rates used in the studies presented here, 0.3–0.5°C/min. However, the large difference in solution volumes used, 2–5 μl (2,3) versus 25 ml, may explain these differences in behavior, because larger undercoolings and supersaturations are possible in the smaller volume elements of the dispersed phase. Droplets formed in the ice matrix decrease in size as the initial solute concentration decreases. For example, in the case of a disodium phosphate solution of initial C_{TP} of 10 mM, more than 90% of the water must freeze for the unfrozen solution to reach a supersaturated state, because the binary eutectic concentration is 110 mM (1,9).

The pH behavior during freezing of buffer solutions reported here is explained by the parameters that affect the kinetics of salt precipitation; specifically, the dependence of the pH at −10°C on the IP of the precipitating ions, which determines the supersaturation. The pH values reached at −10°C show that equilibrium was not achieved during the times that these systems were maintained at this temperature, although a greater extent of salt crystallization may occur with slower cooling rates or longer times at the final temperature.

The presence of indifferent ions in solution, such as $H_2PO_4^-$ may affect the kinetics of precipitation of $Na_2HPO_4 \cdot 12H_2O$. Monosodium dihydrogen phosphate rarely crystallizes under nonequilibrium freezing conditions (2–4). At initial pH values ≤7.4, it is the additive that reaches the highest freeze concentration in sodium phosphate buffers due to its high solubility, reaching 3.42 M at the ternary eutectic temperature of −9.9°C (1). Cavatur and Suryanarayanan (4) have identified the crystalline phases formed during freezing of 300 μl sodium phosphate buffers to −40°C at a rate of ~15°C/min. Their results show that monosodium dihydrogen phosphate above 730 mM reduces the extent of crystallization of $Na_2HPO_4 \cdot 12H_2O$ during freezing of hypereutec-

tic solutions of disodium hydrogen phosphate (190 mM) to −40°C. This behavior has been explained by the high freeze concentrations of sodium dihydrogen phosphate and the resulting high viscosities achieved during freezing of phosphate buffer solutions. High viscosities reduce diffusivity of ions and slow nucleation kinetics of $Na_2HPO_4 \cdot 12H_2O$. Our results indicate that the presence of NaH_2PO_4 at initial concentrations ≤94 mM (activity ≤74 mM) does not inhibit the extent of $Na_2HPO_4 \cdot 12H_2O$ precipitated at −10°C, even though the HPO_4^{2-} concentrations are low (6 mM). Examination of the ion compositions of solutions D and G (Table 1) shows that increasing the $H_2PO_4^-$ concentration 47 times (from 2 to 94 mM), while keeping the HPO_4^{2-} concentration constant (6 mM) increases the $IP_{Na_2HPO_4 \cdot 12H_2O}$ 32 times (from 5.3×10^{-7} to 1.7×10^{-5}). Because of the presence of the common ion (Na^+) in the salts used to prepare the buffer solutions, the concentration of NaH_2PO_4 cannot be varied independent of the supersaturation with respect to $Na_2HPO_4 \cdot 12H_2O$. Compared to the systems we studied, the buffers studied by Cavatur and Suryanarayanan (4) have much higher concentrations of monosodium phosphate, smaller solution volumes, and faster rates of cooling to lower temperatures. All of these factors contribute to delaying the precipitation of $Na_2HPO_4 \cdot 12H_2O$.

Focusing on the molar ratios of phosphate ions while neglecting other factors that regulate salt nucleation can result in misleading generalizations regarding precipitation-induced pH changes during nonequilibrium freezing. For the reasons mentioned above, there is a wide and conflicting range of phosphate molar ratios ($H_2PO_4^-$/HPO_4^{2-}) reported to inhibit the precipitation of $Na_2HPO_4 \cdot 12H_2O$: inhibited at ratios ≥4 (0.73 M/0.19 M) (4) and not inhibited at ratios ≤57 (3.42 M/0.06 M) (1) nor at ratios ≤16 (0.094 M/0.006 M) (this work). Thus, the effects that additives have on salt precipitation and pH during freezing are best analyzed in terms of parameters that regulate the precipitation rate, IP, which is related to the supersaturation, and concentration of nonprecipitating ions which determines the structure and viscosity of the interstitial solution.

CONCLUSIONS

The extent of salt precipitation and pH decreases during nonequilibrium freezing of sodium phosphate buffers to −10°C are smaller than those predicted by the equilibrium behavior. Precipitation-induced pH changes during nonequilibrium freezing are dependent on the variables that regulate the kinetics of salt precipitation: (a) supersaturation and solution composition (concentrations or activities of crystallizing ions, inert ions or other additives); (b) rate at which supersaturation is created; and (c) volume of dispersed droplets of unfrozen solution in the ice matrix.

The effect of solution undercooling on the pH depends on how fast and uniformly the latent heat of crystallization from ice nucleation can be removed from the entire solution volume. Such effects are determined by the combination of volume (or distance to heat sink) and the degree of undercooling. Under the experimental conditions studied, variations in undercooling in the range of 5–12°C did not affect the subsequent changes in pH and salt crystallization.

Although initial pH and initial buffer concentration are useful operational variables, it is difficult to interpret pH-

induced salt precipitation in only these terms because both determine ion concentrations, ion activities, and supersaturations. Moreover, precipitation in these systems occurs from buffer solutions prepared by mixing multiple salts, which lead to nonstoichiometric solution composition. Analysis of pH during freezing to –10°C in terms of ion activity products revealed that (a) pH values at –10°C are weakly dependent on the $IP_{Na_2HPO_4 \cdot 12H_2O}$, and (b) the presence of NaH_2PO_4 at initial concentrations as high as 94 mM does not affect the extent of $Na_2HPO_4 \cdot 12H_2O$ precipitated (pH) at –10°C, even though the HPO_4^{2-} concentrations were low.

Results of studies of sodium phosphate precipitation from various laboratories are compared and differences are explained by considering the cooling rates, solution volumes, and ion concentrations. Larger undercoolings and higher ion concentrations are required for precipitation of $Na_2HPO_4 \cdot 12H_2O$ in smaller volumes.

Although the results of this research are limited to temperatures above –10°C, the above generalizations should also be valid in freeze-drying applications where the final temperature in freezing is often –40°C and freezing times are on the order of several hours. The pH changes in a freeze-drying environment will generally be slightly greater because lower temperatures mean greater supersaturation and longer times mean more time for crystallization. However, it must be recognized that as the temperature lowers and freeze concentration increases, viscosity increases will slow the rate of crystallization. Thus, the magnitude of the pH changes will likely not differ greatly from those reported in this work unless holding times in the frozen state are much longer than typical freeze-drying operations. Finally, it must be emphasized that addition of other components, i.e., drug and other excipients, may dramatically alter buffer crystallization and resulting pH shifts. These effects will be addressed in future reports.

ACKNOWLEDGMENTS

REFERENCES

1. L. van den Berg. The effect of addition of sodium and potassium chloride to the reciprocal system: KH_2PO_4–Na_2HPO_4–H_2O on pH and composition during freezing. *Arch. Biochem. Biophys.* **84**:305–315 (1959).
2. N. Murase and F. Franks. Salt precipitation during the freeze-concentration of phosphate buffer solutions. *Biophys. Chem.* **34**:293–300 (1989).
3. N. Murase, P. Echlin, and F. Franks. The structural states of freeze-concentrated and freeze-dried phosphates studied by scanning electron-microscopy and differential scanning calorimetry. *Cryobiology* **28**:364–375 (1991).
4. R. K. Cavatur and R. Suryanarayanan. Characterization of frozen aqueous solutions by low temperature X-ray powder diffractometry. *Pharm. Res.* **15**:194–199 (1998).
5. M. J. Pikal. Freeze-drying of proteins—Part II: Formulation selection. *BioPharm.* **4**:26–30 (1990).
6. M. W. Towsend and P. P. DeLuca. Use of lyoprotectants in the freeze-drying of a model protein, ribonuclease A. *J. Parenter. Sci. Technol.* **42**:190–199 (1988).
7. S. S. Larsen. Studies on stability of drugs in frozen systems IV: The stability of benzylpenicillin sodium in frozen aqueous solutions. *Dansk. Tidsskr. Farm.* **45**:307–316 (1971).
8. M. P. W. te Booy, R. A. de Ruiter, and A. L. J. de Meere. Evaluation of the physical stability of freeze-dried sucrose-containing formulations by differential scanning calorimetry. *Pharm. Res.* **9**:109–114 (1992).
9. L. van den Berg. pH changes in buffers and foods during freezing and subsequent storage. *Cryobiology* **3**:236–242 (1966).
10. S. S. Larsen. Studies on stability of drugs in frozen systems VI: The effect of freezing upon pH for buffered aqueous solutions. *Arch. Pharm. Chem. Sci. Ed.* **1**:41–53 (1973).
11. A. P. MacKenzie. Non-equilibrium freezing behaviour of aqueous systems. *Phil. Trans. R. Soc. London. B* **278**:167–189 (1977).
12. M. J. Taylor. Physico-chemical principles in low temperature biology. In B. W. W. Grout and G. J. Morris (eds.), *The Effects of Low Temperatures on Biological Systems,* E. Arnold, London, 1987, pp.1–71.
13. A. E. Nielsen and J. M. Toft. Electrolyte Crystal Growth Kinetics. *J. Cryst. Growth* **67**:278–288 (1984).
14. I. López-Valero, C. Gómez-Lorente, and R. Boistelle. Effects of sodium and ammonium ions on occurrence, evolution and crystallinity of calcium phosphates. *J. Cryst. Growth* **121**:297–304 (1992).
15. O. Söhnel and J. Garside. *Precipitation: Basic Principles and Industrial Applications,* Butterworth-Heinemann Ltd., Oxford, 1992.
16. H. Galster. *pH Measurement,* VCH, New York, 1991, pp.121–123.
17. H. Galster. *pH Measurement,* VCH, New York, 1991, pp.156–162.
18. W. Kurz and D. J. Fisher. *Fundamentals of Solidification,* Trans Tech Publications Ltd., Switzerland, 1986.
19. A. E. Nielsen. Electrolyte crystal growth mechanisms. *J. Cryst. Growth* **67**:289–310 (1984).
20. R. Boistelle and J. P. Astier. Crystallization mechanisms in solution. *J. Cryst. Growth* **90**:14–30 (1988).
21. Y. K. Kharaka, E. H. Perkins, W. D. Gunter, and J. D. Debraal. Geochemical modeling of water-rock interactions using SOLMINEQ-88. *884227 US Geol. Surv.* (1988).
22. E. H. Perkins, Y. K. Kharaka, W. D. Gunter, and J. D. Debraal. Geochemical modeling of water-rock interactions using Sol-mineq-88. *ACS Symp. Ser.* **416**:117–127 (1990).
23. G. Gómez. *Crystallization-Related pH Changes During Freezing of Sodium Phosphate Buffer Solutions,* Ph.D. Thesis, University of Michigan, Ann Arbor, Michigan, 1995.
24. C. Körber. Phenomena at the advancing ice liquid interface - solutes, particles and biological cells. *Q. Rev. Biophys.* **21**:229–298 (1988).
25. M. Kochs, C. Körber, B. Nunner, and I. Heschel. The influence of the freezing process on vapor transport during sublimation in vacuum-freeze-drying. *Int. J. Heat Mass Transfer* **34**:2395–2408 (1991).
26. M. Jochem, U. Hartman, and C. Korber. Modeling of coupled heat and mass transfer problem of nonplanar solidification and melting in aqueous solutions and numerical treatment. In K. D. Diller (ed.), *Network Thermodynamics, Heat and Mass Transfer in Biotechnology,* American Society of Mechanical Engineers, New York, 1987, pp.73–80.
27. J. H. Perepezko. Kinetic processes in undercooled melts. *Mater. Sci. Eng., A* **226**:374–382 (1997).
28. S. Ganguly and K. S. Adiseshaiah. Ice nucleation in emulsified aqueous salt-solutions—A differential scanning calorimetry study. *Colloids Surf.* **66**:105–111 (1992).
29. D. Clausse, I. Sifrini, and J. P. Dumas. On the study by DSC of the unexpected ice melting at 0°C of emulsified aqueous saline solutions. *Thermochim. Acta* **122**:123–133 (1987).
30. R. J. Davey, A. M. Hilton, and J. Garside. Crystallization from oil in water emulsions: particle synthesis and purification of molecular materials. *Chem. Eng. Res. Design* **75**:245–251 (1997).